

# Hot Magnetic Stars Abundances, Spectroscopy, Photometry, Systematics.

K. Hunger  
Kiel

## Systematics

The present discussion of hot magnetic CP stars is restricted to  $17000 \text{ K} < T_{\text{eff}} < 30\,000 \text{ K}$ , the upper limit being the temperature up to which magnetic fields can be observed, the lower limit defining the boundary between He-rich and He-poor stars.

All of the hot magnetics belong to the class of intermediate helium stars which is defined by  $n_{\text{H}}/n_{\text{He}} < 3$  (number ratio, Hunger 1975). Walborn (1983) lists 23 stars of this class, mostly with  $n_{\text{H}}/n_{\text{He}} \approx 1$ , and of spectral type B2 V. Magnetic fields, so far, have been discovered in 7 of them (Borra et al. 1983). All but one of these are spectrum variables, with periods  $0.9 < P/\text{day} < 1.7$  (except one with  $P = 9.5 \text{ d}$ ), (Pedersen, 1979) and with rotational velocities of the order of  $v \sin i \approx 150 \text{ km/s}$  which are compatible with the  $(P, v \sin i)$ -relation of stars near the main sequence; i.e. these stars are oblique rotators.

As to the age and population: all evidence points to a rather young population as a large fraction is found in the Orion aggregate and the young cluster IC2944. The masses are well in excess of one solar mass, in contrast to the (old) extreme helium stars. Also the metal content of the subgroup seems to be solar (within a factor of 2) (Hunger, 1975).

## Masses

The masses are crucial when one wants to know whether He-enrichment in the hot magnetics is due to diffusion and hence is confined to the surface, or whether the entire star is enriched, as is believed for the class of extreme helium stars. Since no binaries among this class are known, the only way to determine the mass is spectroscopical: from the distance  $d$  and the  $V$ -magnitude, the luminosity  $L = 4 \pi R^2 \sigma T_{\text{eff}}^4$  is derived.  $T_{\text{eff}}$  is obtained from spectral analysis, and hence the radius  $R$ , likewise the gravity  $g = GM/R^2$ , and hence the mass  $M$ .

The best way today to determine  $T_{\text{eff}}$  is from IUE fluxes, as the main flux of a B-star is carried in the IUE-band (Remie and Lamers, 1982). The fluxes are determined with a precision of + 10%, and hence  $T_{\text{eff}}$  with + 2.5%. As an example, the results for the best studied hot CP star,  $\sigma$  Ori E is given (Groote and Hunger, 1982):  $T_{\text{eff}} = 22500 \text{ K} + 600 \text{ K}$ , independent of phase. In Fig. 1, the observed and theoretical fluxes are reproduced, which well agree, except for the IR-excess we come later to. While  $T_{\text{eff}}$  is determined largely independently of gravity  $g$  and of the helium number fraction  $\epsilon_{\text{He}}$ ,  $g$  and  $\epsilon_{\text{He}}$  have to be determined

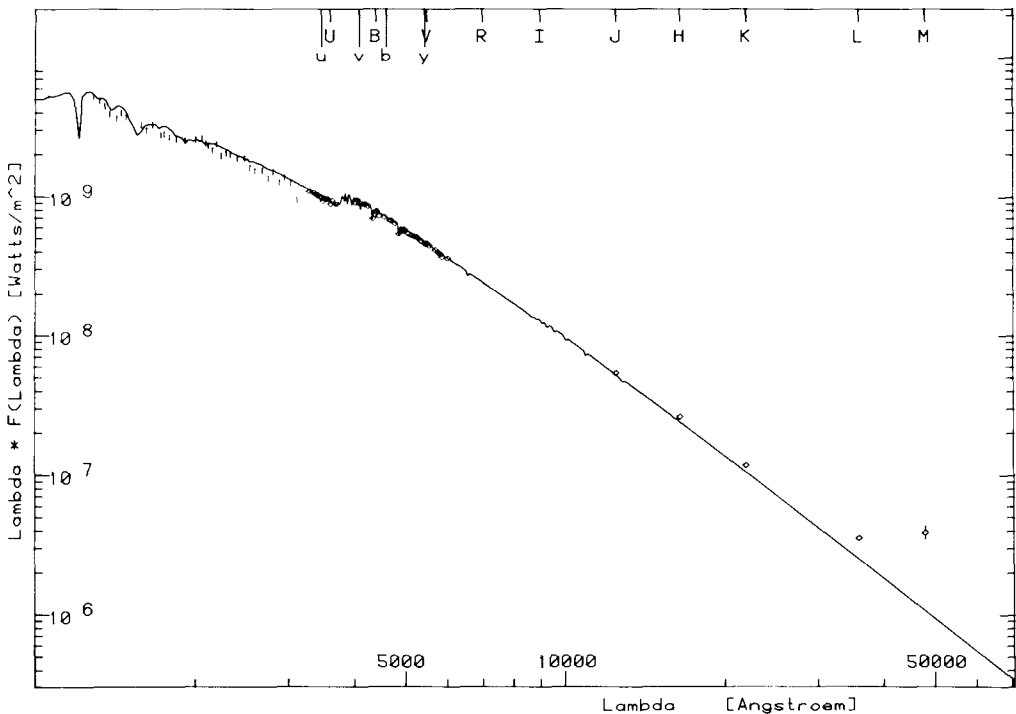


Fig. 1: The flux of  $\sigma$  Ori E, from 1100 Å to 50000 Å

simultaneously, from the profiles of the Balmer and helium lines, and of course phase dependent, as  $\sigma$  Ori E is a helium variable. The result is shown in Fig. 2: gravity is nearly constant,  $\log g = 3.85$ , while  $\epsilon_{\text{He}}$  reflects the familiar behaviour of the R-index variations (Pedersen, and Thomsen, 1977). With  $d = 400$  pc (Heintz, 1974), the mass finally results:  $M = 3 M_{\odot}$ .

Mass and gravity come out uncomfortably small. Both values consistently correspond to a star which evolved from a helium rich main sequence, with  $X = 0.3$  (Fig. 3). However, a young star that begins its life as a fully mixed helium star is hardly conceivable, and hence the results have been questioned (Walborn, 1983). Either the distance is underestimated - which is rather unlikely - or the equivalent widths used are systematically too small. The ESO plate calibration has been carefully checked by intercomparison with other photographic systems and has been found reliable. The intercomparison, however, was purely photographic, and it may turn out that photoelectrically determined equivalent widths turn out to be systematically larger. A first indication for this comes from ESO CASPEC CCD spectrograms which for faint stars ( $V = 10^m$ ) yield equivalent widths that are larger by

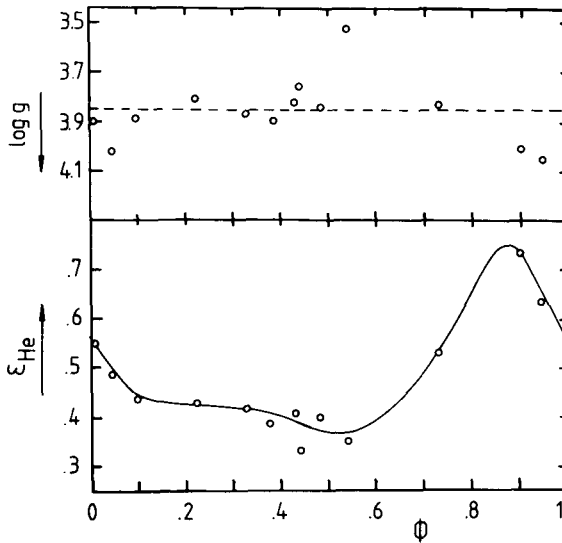


Fig. 2:  
Gravity and helium  
number fraction of  
 $\sigma$  Ori E, as function  
of phase

40% in some cases. If this also holds for a bright star like  $\sigma$  Ori E, then gravity has to be corrected by a factor of more than 2 which means that the mass is  $7 M_{\odot}$  rather than  $3 M_{\odot}$ , gravity and mass now well in agreement with the normal composition main sequence. Helium enrichment then is only confined to the surface.

#### The Oblique Rotator.

The variation of the helium content with phase can best be understood on the basis of an oblique rotator. The problem with the helium strong magnetic variables however, is that one does not observe variations of the radial velocities when the helium rich parts of the surface approach the observer or when they recede (Groote and Hunger, 1977). The missing radial velocities ( $\Delta v_{\text{Rad}} < + 2 \text{ km/s}$ ) have some authors led to believe in helium-rich bands rather than helium-rich caps (Shore and Adelman, 1981; Bolton, 1983). While this may be true in exceptional cases, it is certainly not true in the case of  $\sigma$  Ori E, for if one invents a surface structure that leads to small amplitudes in  $v_{\text{Rad}}$ , then one inevitably ends up also with small amplitudes in the equivalent widths. The answer to this problem is saturation. If the helium lines are core saturated both in the cap and in the disk, as is the case in our sample of stars, then the radial velocities seem to reflect rather the motion of the disk, because the disk lines are narrow, than the motion of the cap. This has been shown rigorously by Gruschinske (see Groote and Hunger, 1982) for the idealized case of a single helium cap that covers a full hemisphere of the star. The helium abundance inside and outside the cap is taken from Fig. 2, and  $v \sin i = 150 \text{ km/s}$  is assumed. The two phases, when the boundary is subsolar,

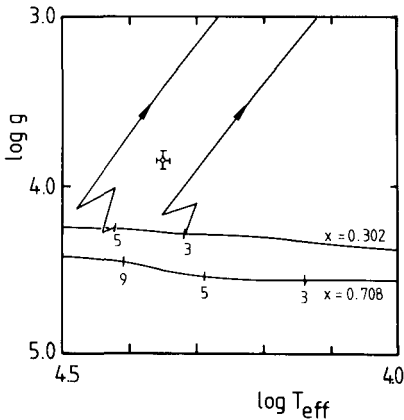


Fig. 3:

Two main sequences, with the hydrogen mass fractions  $X = 0.302$  and  $0.708$  (normal composition), and two evolutionary tracks, of 3 and 5 solar mass stars, are shown in the  $(g, T_{\text{eff}})$ -diagram.

and when the cap is either approaching or receding is shown in Fig. 4. The example is the (symmetrized) profile of HeI 4471. While the wings (or equivalently the core of weak lines) indeed are shifted to the blue when the cap is approaching, the core is shifted inversely, by an amount of 40 km/s.

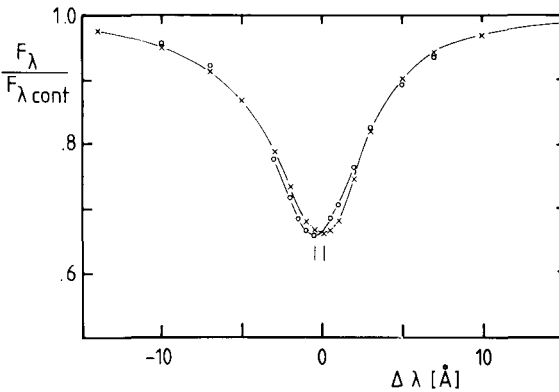


Fig. 4:

The symmetrized profile of HeI 4471, in two phases:  $\times \times \times$  helium cap is approaching,  $o o o$  helium cap is receding. The core is shifted inversely, by 40 km/s.

This unexpected behaviour is indeed observed, without any exception, in all of the HeI lines, (Fig. 5). The (saturated) strong lines  $\lambda\lambda$  3820, 4026, 4471 have inversely shifted cores, the (unsaturated) weak lines 4121, 4438, 4713 are directly shifted, while the intermediate lines 4009, 4144, 4388 are unshifted. This explains why correlation techniques (Groote and Hunger, 1977) which use averages over many lines do not reveal R.V. amplitudes. Interesting in this context is that some He weak magnetic variables with their unsaturated lines do show R.V. variations.

An example for a banded structure represents HD 37776, where, for the first time, a magnetic quadrupole field with current loops has been discovered, Fig. 6 (Thompson and Landstreet, 1985; Groote and Kaufmann, 1981).

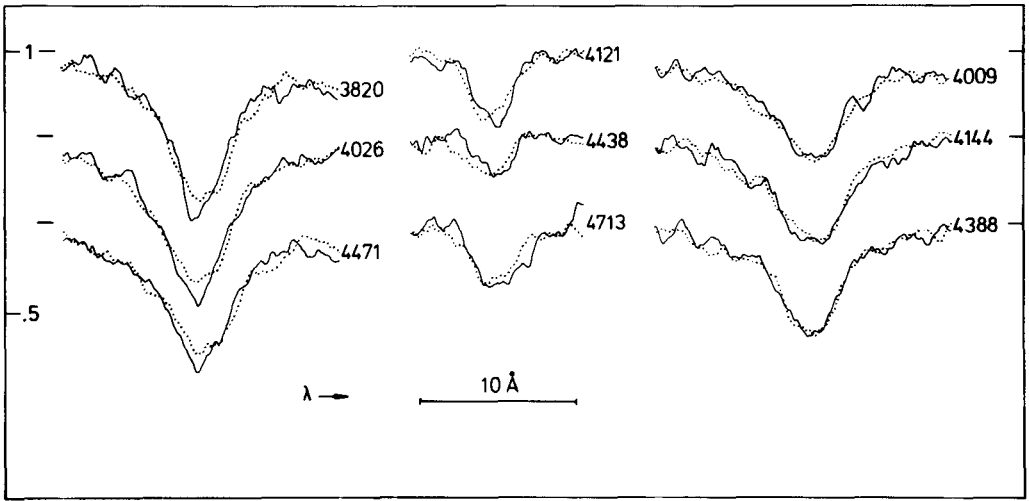


Fig. 5: Profiles of strong, medium strong and faint He lines of  $\sigma$  Ori E in two phases: ..... helium cap is approaching, — helium cap is receding. Cores of strong lines are inversely shifted, while faint lines are directly shifted.

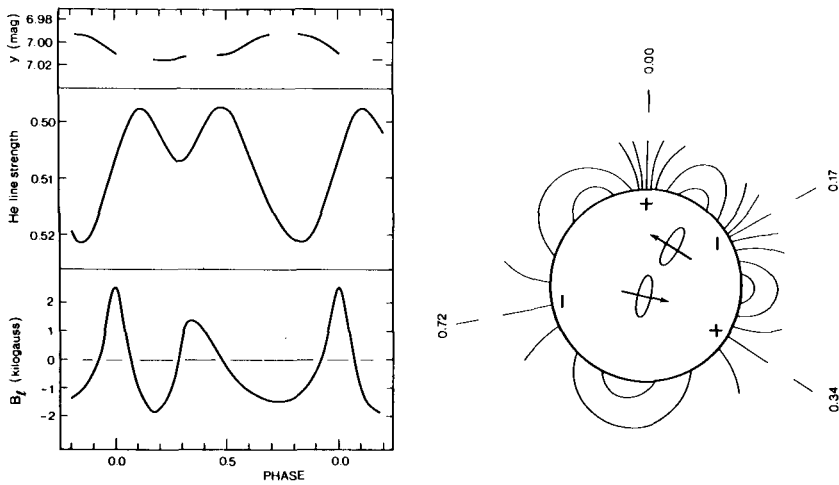


Fig. 6: Phase variation of  $y$ , He line strength and magnetic field of HD 37776. This variability is best explained by a banded helium distribution that is tied to a magnetic quadrupole field (Thompson and Landstreet, 1985).

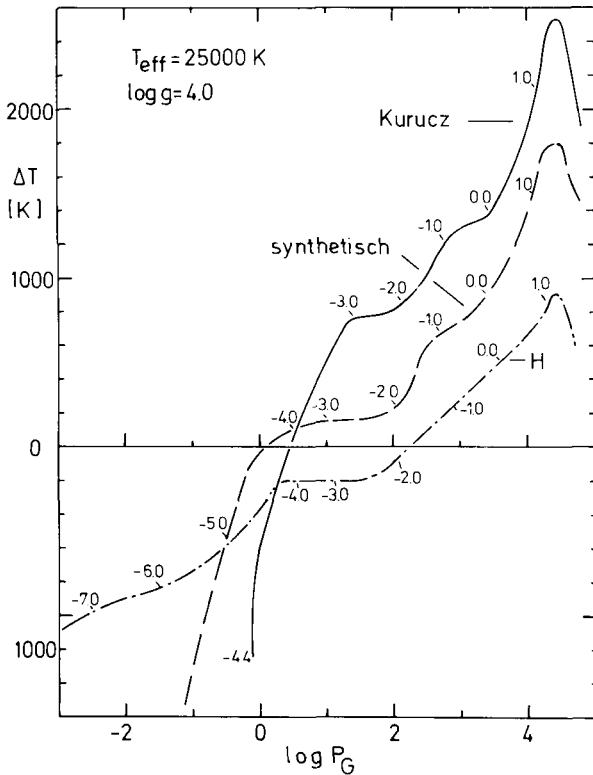


Fig. 7:  
The temperature differences vs. an unblanketed model atmosphere, as function of depth ( $P_g$ ):  
- · - · - only H-line blanketing, - - - additional 500 metal lines, and — full line blanketing. The temperature gradient is similar in all blanketed models.

### Atmospheric Models

How realistic are the model atmospheres so far in use? For, in the hot magnetic CP's we encounter the following problems:

- 1) metal line blanketing
- 2) horizontal abundance variations
- 3) vertical abundance stratifications
- 4) influence of magnetic fields on structure and spectrum

1) Fully blanketed models are available only for normal compositions (Kurucz, 1979). For He-enriched atmospheres, only a few models exist which moreover include "only" up to 500 metal lines (Heber, 1979). The effect of metal line blanketing on the temperature and hence on the emergent spectrum can best be judged from Fig. 7, where the temperature differences with respect to an unblanketed model are shown: for a Kurucz-model, for a Heber-model, and for a H-line blanketed model. For the same effective temperature, the temperature increases in the region of spectrum formation from the unblanketed model by 300 K (H-lines), by 700 K (500 metal lines), and lastly by 1300 K (full set of lines). The slopes of the 3 blanketed models, however, remain similar which means that the emergent fluxes, continua as well as lines, come out alike. Hence H-line blanketed models can safely be used, if one only corrects

$T_{\text{eff}}$  by  $-1000$  K. The latter was shown for normal composition atmospheres. It holds also for He-enriched atmospheres, as long as  $\epsilon_{\text{He}} < 0.5$ .

2) Horizontal abundance variations, namely the variation of helium in spots (bands) and disk, do not pose any problems, as long as  $T_{\text{eff}}$  and  $g$  are constant over the surface: if one adds the line profiles of spots (bands) and disk, weighted with the appropriate surface area fractions, then a profile results which is indistinguishable from a line profile with a helium content that is the area mean of the two helium fractions, of spots (bands) and disk.

It has been claimed that the sometimes observed antiphase variation of silicon does not reflect abundance variations, but is due to differences in excitation and ionization between disk to spot (see Bolton, 1983). This has been checked by Heber (1985), for the case of  $\checkmark$  Ori E, on the basis of metal line blanketed atmospheres. The result is that the lines of Si III  $\lambda\lambda$  4128, 4131 increase by 6% in equivalent widths, when going from the disk ( $\epsilon_{\text{He}} = 0.35$ ) to the spot ( $\epsilon_{\text{He}} = 0.90$ ), while Si III  $\lambda\lambda$  4553, 4568, 4575 decrease by 5%. Somewhat larger is the increase for Si III  $\lambda$  1417: 19%. This means that the silicon variations, if real, are due to abundance variations.

3) Vertical abundance stratifications are to be expected on account of diffusion. Other than in the case of compact stars like white dwarfs, in hot CP's helium floats atop of hydrogen. Whether the temperature structure is affected by such a "chemical profile" (which presumably is a diffusive "profile"), and whether the spectral lines will be affected depends not only on the strength of the discontinuity, but much more so on the depth of transition. If this depth is in the intermediate range of  $\tau_{4000} = 10^2 \dots 1$ , then, from the calculations performed for white dwarfs (Jordan, 1985), models with temperature inversions and correspondingly strange line profiles occur. Analogous calculations for hot CP stars are still pending. But from the foregoing results one can extrapolate: as long as the line profiles are not anomalous, one can be fairly sure, that the transition depth is below  $\tau_{4000} = 1$ , and that the spectral analysis hence yields parameters and abundances of the chemically homogeneous part of the atmosphere, above the transition.

Anomalous profiles, i.e. profiles that cannot be reproduced by any conceivable model and any reasonable rotational velocity, are observed in the helium variable HD 49333. The intermediate temperature ( $T_{\text{eff}} = 15700$  K) CP variable is depleted in helium which means that helium is diffused downwards, while hydrogen floats atop, similarly as in white dwarfs. Kaufmann and Theil (1985) have calculated profiles, assuming various abundance steps (strength of discontinuity), and various depths of transition. In Fig. 8a, the helium number fraction above the transition is taken as  $\epsilon_{\text{He}} = 0.001$  and  $0.01$  resp., while  $\epsilon_{\text{He}}$  below the transition is  $0.12$ . The depth of transition is kept at  $\tau_{4000} = 0.8$ . (The model atmosphere, however, has been computed with the

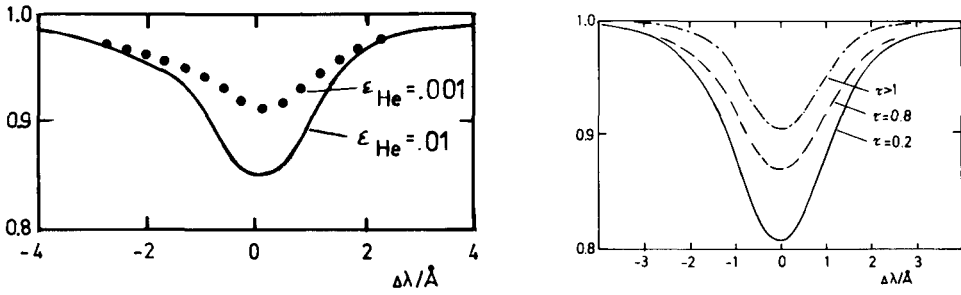


Fig. 8: How a vertical abundance stratification influences the profiles

- a) at  $\tau_{4000} = 0.8$ , the composition changes from  $\epsilon_{\text{He}} = 0.001$  (....) and  $0.01$  (—) resp. to  $\epsilon_{\text{He}} = 0.12$  of the bottom layer. (4471)
- b) The composition above the transition depth varies from  $\tau = 0.2$  to  $0.8$  and  $>1$  (homogeneous model). (He I 4388)

assumption of an homogeneous atmosphere with  $\epsilon_{\text{He}} = 0.12$ , as in this case the inhomogeneity has little effect on the model.) The reduction of helium in the upper layer reduces the core of HeI 4471, whereas the wings are not affected, i.e. the line appears shallow. In Fig. 8b, the effect of the depth of transition is shown: the transition from  $\epsilon_{\text{He}} = 0.02$  (above) to  $\epsilon_{\text{He}} = 0.12$  (below) takes place at  $\tau_{4000} = 0.2$  and  $0.8$  resp. HeI  $\lambda$  4388 is greatly reduced when the transition depth moves downwards. In Fig. 8c, finally, the observed profile is compared with what is considered the best combination of depth of transition and strength of transition:  $\epsilon_{\text{He}} = 0.001$  (above) and  $0.20$  (below) with  $\tau_{4000} = 0.4$ . (These results are provisional as they are based on noisy IIAO-plates. Furthermore, the surface flux integration effect - see above - is neglected.)

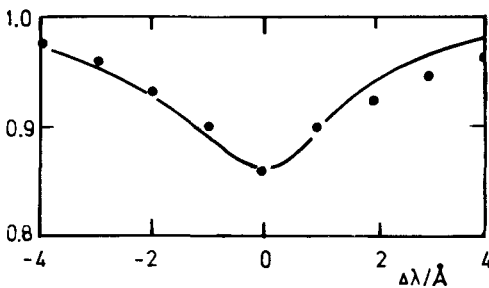


Fig. 8c: The observed profile ( . . . ) of HD 49333 is best reproduced by a model with a transition depth at  $\tau_{4000} = 0.4$ , and with  $\epsilon_{\text{He}} = 0.001$  (surface layer) and  $0.20$  (bottom layer) resp.

4) How the electromagnetic field influences the atmospheric structure and the emergent spectrum, via the opacity (Zeeman splitting of the contributing atomic lines) and via the magnetic forces (pressure stratification) has been studied in detail by Carpenter (1985) (see also Madej, 1981). The effects on the line profiles, however, are



small, and can only be detected under exceptional conditions (magnetic fields of the order of 20 KG, high quality spectrograms).

### The Shell

Hot magnetic stars are believed to have corotating magnetospheres. In the example of  $\sigma$  Ori E it is shown that the magnetosphere is reduced to a truncated Van Allen belt (two corotating clouds) that contain a (predominantly) hydrogen plasma at a temperature of 15 000 K (Groote and Hunger, 1982). These clouds account for most of the variable features observed. (Even the eclipse like features of the light curve are due to the two corotating clouds. The conjecture that the brightness decline in the u-band is due to the helium caps, see Bolton, 1983, is erroneous as the helium caps are even (slightly) brighter than the disk, by  $\Delta u = 0.^m1$ , Kaufmann and Theil, 1985.)

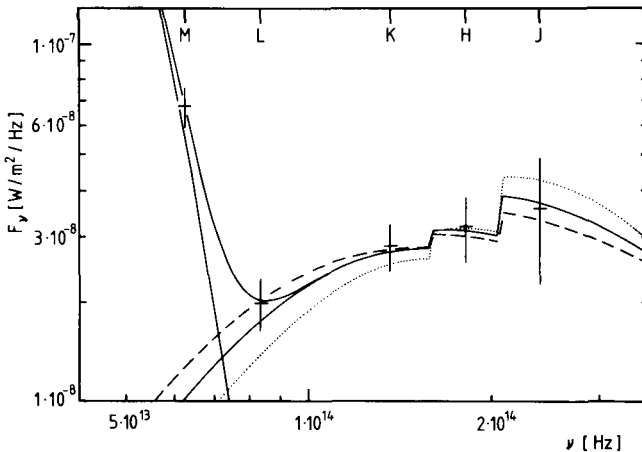


Fig. 9:  
The infrared excess of  $\sigma$  Ori E. Observations are marked by (long) crosses. The full drawn curve (lower part of the diagram) corresponds to free emission, with  $T = 15000$  K.

The temperature of the clouds is derived from the IR excess up to the L-band. The additional excess at the M-band (Fig. 9) has often been questioned as the idea of corotating grains in the vicinity of a hot star is hardly conceivable. Also the excess could not be confirmed (Bonsack and Dyck, 1983; Odell and Lebofsky, 1984). If the excess were real, an alternative explanation would be synchrotron radiation due energetic particles (Havnes, 1981). In this case, radio emission should be observable. Attempts to detect emission with the 100 m Effelsberg telescope at 2 cm failed, because the spatial resolution was insufficient (see Groote and Hunger, 1982). At last  $\sigma$  Ori E, though, was detected at 2 and 6 cm, with the VLA - it was a serendipitous discovery (Drake et al., 1985). Also IRAS was able to see  $\sigma$  Ori E, the resolution however being too small to definitely ascribe it to the component E (Walker, 1985). These discoveries certainly open up the discussion of the M-band excess.

### Magnetospheres and Winds

A major campagne has been started (Barker et al. 1985) to contemporaneously follow the observations in the optical, UV and Zeeman polarization, in order to study the interaction of winds with magnetic fields. A first example is the helium rich HD 184927. Fig. 10, left panel shows the variable features which have a common period of 9.5 days. The right panel reproduces the CIV resonance doublet at 5 different phases. The profiles vary with the same period: maximum (red shifted) emission occurs when the magnetic pole is subsolar, while maximum absorption occurs when the equator is subsolar. A detailed model is still lacking. It is evident, however, that the wind is strongly modulated by the magnetic field.

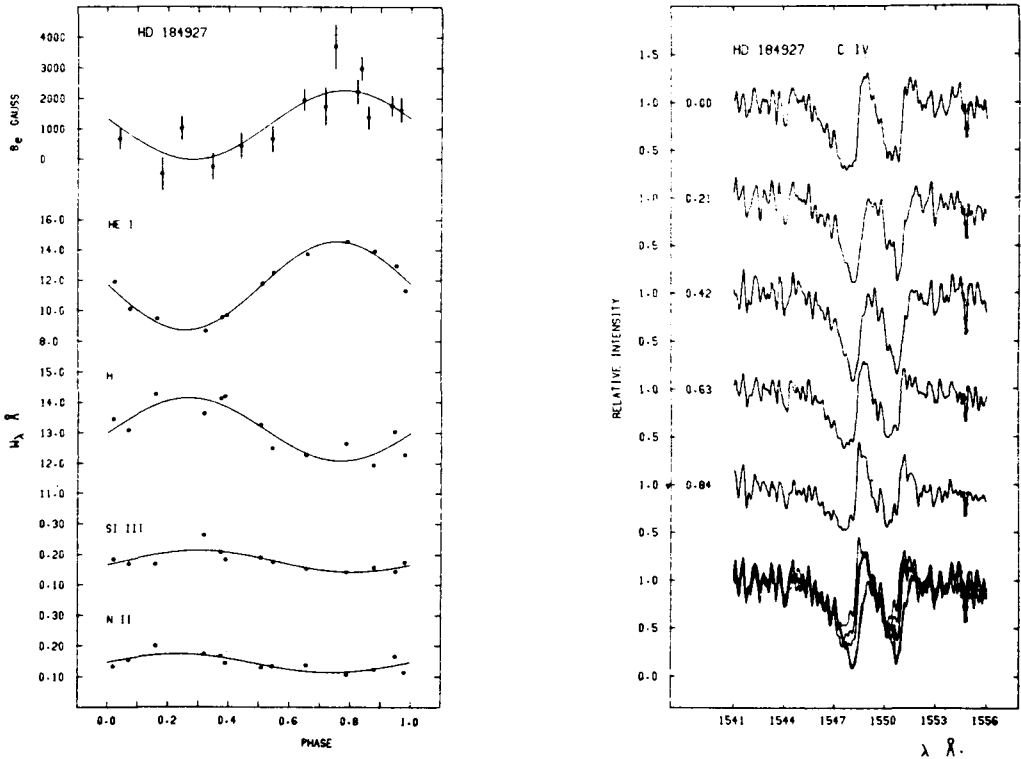


Fig. 10: The phase variation of HD 184927. Left panel: magnetic field, line strengths of He, H, Si III and N II (from top to bottom). Right panel: the resonance doublet of CIV, for various phases (left hand scale), and all phases superimposed, at the bottom (Barker et al. 1985).

Altogether, 8 helium strong stars have been checked for magnetically controlled winds, again CIV being the strongest indicator (Barker et al., 1985). A strange correlation has been found: the fast rotators do not show CIV in emission, but show  $H_{\alpha}$ -emission instead, while for the slow rotators the opposite seems to be true (Fig. 11). More observations are needed before one can work out a definite model.

A similar campagne was started to observe helium weak variables, the first example being HD 21699 (Brown et al., 1985). Again, the CIV resonance doublet was found variable, with a period of 2.5 d, which is also the period of the magnetic field. In this case a model is forwarded. The approach however, is complicated, as the geometry in case of a strong magnetic field deviates from sphericity. In the case of HD21699, the wind occurs in form of a single jet or plume over one of the magnetic poles. It appears, though, that probably more work is

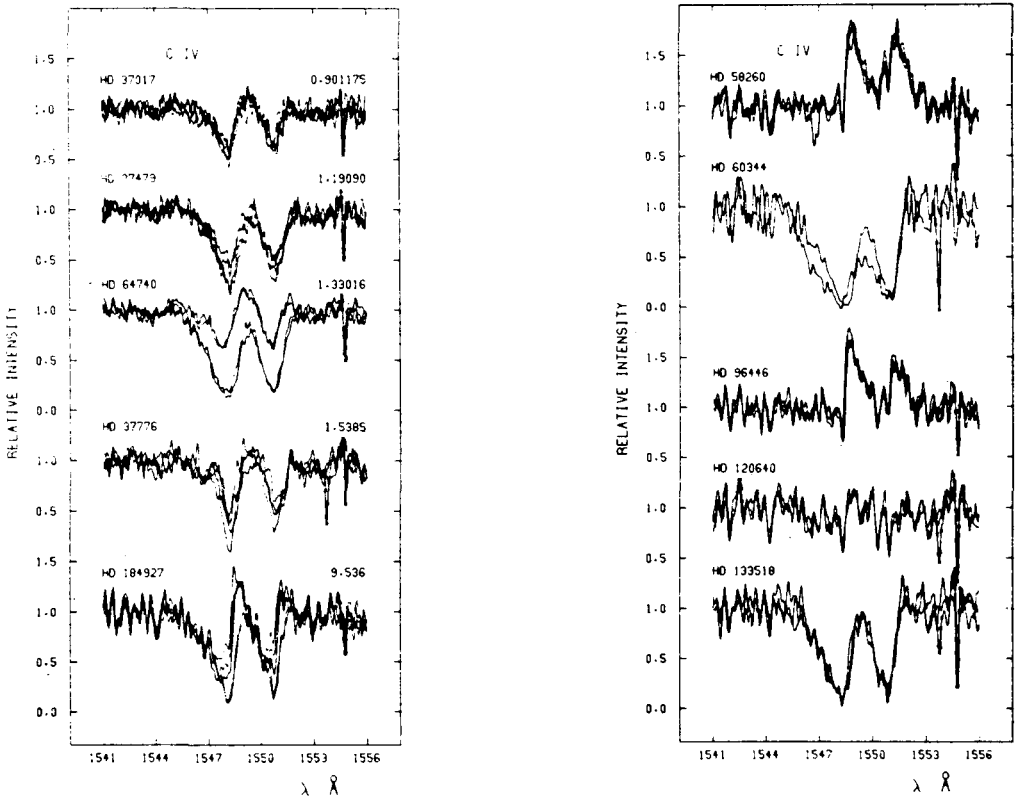


Fig. 11: Fast rotators (left panel) hardly show C IV in emission, while for the slow rotators (right panel) the opposite seems to be true (Barker et al. 1985).

needed, observational and theoretical, to corroborate this result. Of special importance in this context may be the large number of high resolution IUE spectrograms of  $\epsilon$  Ori E which cover all crucial phases and which still wait unused in the databank of VILSPA.

### Theory

This review cannot end without at least mentioning the important work done in the difficult field of modelling magnetospheric plasmas around early type stars. Some promising progress has been made by Havnes and Goertz (1984), but time does not permit discussion. When in the end, a selfconsistent picture of the structure of the magnetic field, of the magnetosphere and of the magnetically controlled wind around an early B type star emerges, it may be possible to make predictions as to magnetospheres of still hotter stars like O stars where magnetic fields cannot be observed, but which nevertheless may also have magnetically controlled winds.

### References

- Barker, P., Brown, D.N., Bolton, C.T. and Landstreet, J.D.: 1985, preprint
- Bolton, C.T.: 1983, *Harv. Obs. Bull.* 7, 241
- Bonsack, W.K. and Dyck, H.M.: 1983, *Astron. Astrophys.* 125, 29
- Borra, E.F., Landstreet, J.D. and Thompson, I.: 1983, *Astrophys. J. Suppl.* 53, 151
- Brown, D.N., Shore, S.N. and Sonneborn, G.: 1985, *Astron. J.*, in press
- Carpenter, K.G.: 1985, *Astrophys. J.* 289, 660
- Drake, S.A., Abbot, D.C., Bieging, J.H., Churchwell, E. and Linsky, J.L.: 1985
- Groote, D., and Hunger, K.: 1977, *Astron. Astrophys.* 56, 129
- Groote, D., and Hunger, K.: 1982, *Astron. Astrophys.* 116, 64
- Groote, D. and Kaufmann, J.P.: 1981, in *The Chemically Peculiar Stars of the Upper Main Sequence*, 23rd Liège Astrophysical Colloquium, p. 435
- Havnes, O.: 1981, in *The Chemically Peculiar Stars of the Upper Main Sequence*, 23rd Liège Astrophysical Colloquium, p. 403
- Havnes, O. and Goertz, C.K.: 1984, *Astron. Astrophys.* 138, 421
- Heber, U.: 1979, Diploma Thesis
- Heber, U.: 1985, private communication
- Heintz, W.D.: 1974, *Astrophys. J.* 79, 397
- Hunger, K.: 1975, in *Problems in Stellar Atmosphere and Envelopes*, Baschek, Kegel and Traving Editors, Springer-Verlag Berlin Heidelberg New York, p. 57
- Jordan, S.: 1985, private communication
- Kaufmann, J.P. and Theil, U.: 1985, private communication
- Kurucz, R.L.: 1979, *Astrophys. J. Suppl.* 40, 1

- Madej, J.: 1981, in *The Chemical Peculiar Stars of the Upper Main Sequence*, 23rd Liège Astrophysical Colloquium, p. 379
- Odell, A.P. and Lebofsky, M.: 1984, *Astron. Astrophys.* 140, 468
- Pedersen, H.: 1979, *Astron. Astrophys. J. Suppl.* 35, 313
- Pedersen, H. and Thomsen, B.: 1977, *Astron. Astrophys. Suppl.* 30, 11
- Remie, H. and Lamers, H.J.G.L.M.: 1982, *Astron. Astrophys.* 105, 85
- Shore, S.N. and Adelman, S.: 1981, in *The Chemically Peculiar Stars of the Upper Main Sequence*, 23rd Liège Astrophysics Colloquium, p. 429
- Thompson, I.B. and Landstreet, J.D.: 1985, *Astrophys. J.* in press
- Walborn, N.: 1983, *Astrophys. J.* 268, 195
- Walker, H.J.: 1985, preprint